Universidad Complutense de Madrid

Facultad de Ciencias Físicas

Departamento de Física de la Tierra y Astrofísica

Impacto de la resolución en la representación de la variabilidad climática del Atlántico norte: causas y teleconexiones

Impact of model resolution on the representation of the North Atlantic climate variability: drivers and teleconnections

Trabajo Fin de Máster

Máster en Meteorología y Geofísica

Presentado por:

Guillermo Sanz Arranz

Directores:

Pablo Ortega Montilla, Eduardo Moreno Chamarro, María Luisa Montoya Redondo

Curso 2018/2019

Abstract

The Atlantic Ocean plays an important role in the Earth's climate specially through its interactions with the atmoshphere during the boreal winter. There is when a great atmospheric phenomenon as the North Atlantic Oscillation (NAO) influences the deep water formation in the North Atlantic, getting to control the intensity of the Atlantic Meridional Overturning Circulation (AMOC). Interannual NAO variability can thus induce lower frequency variability of the AMOC. This brings with it a possible important role of the model resolution used for the detection of the mechanisms responsible for AMOC variations as well as in the link between the Atlantic Multidecadal Variability (AMV) and the AMOC. In this work in particular, we will get to assess two different resolutions of the model used and later to found that the lower resolution is more able to distinguish the main drivers of AMOC variability and their response to both oceanic and atmospheric influences in a multidecadal approach. This will help to study the concrete teleconnections of the AMV index with the temperatures over concrete areas as North America and Western Europe and with the precipitations in the Sahel.

1 Introduction

The circulation in the Atlantic Ocean is generally described in terms of the so-called Atlantic Meridional Overturning Circulation (AMOC). The AMOC can be subdivided into four branches: deep water formation (DWF) at high latitudes, upwelling of deep water masses, and surface and deep currents closing the loop (Kuhlbrodt et al, 2007). These branches span the entire Atlantic basin on both hemispheres, forming two overturning cells, a deep one with North Atlantic Deep Water (NADW) and an abyssal one with Antarctic Bottom Water (AABW).

NADW and AABW are formed in regions of high surface density in the North Atlantic and in the Southern Ocean, respectively. In the North Atlantic, DWF is formed through deep ocean convection of up to 2000 m in the Labrador Sea driven by cooling in winter (Marshall and Schott, 1999); in the Nordic and Greenland Seas open ocean convection occurs less frequently and is generally shallower. The driving mechanism

is also different, with surface density increasing through brine rejection during sea-ice formation in winter. In the Southern Ocean, DWF takes place mainly along the continental slope of Antarctica. In winter, dense near-surface water is created through brine release during sea-ice formation and strong heat loss in polynyas. This dense waters sinks to the bottom of the continental shelf and flows down the continental slope; together with the entrainment of ambient waters this leads to bottom water formation (Baines and Condie, 1998), creating the densest and coldest water of the deep ocean, which spreads through the South Atlantic western basins northward into the North Atlantic.

Deep-water upwelling can occur in two different ways. On one hand, wind- and buoyancy-driven mixing in the ocean surface layer, instabilities driven by large-scale shear and breaking of internal waves generated through winds and tides in the ocean interior, and frictionally-driven processes at the bottom boundary all induce turbulent

mixing which helps to pump heat from the atmospheric boundary layer into the deep ocean, which thereby gain buoyancy. This leads to diapycnal mixing, which dominates at low latitudes. On the other hand, upwelling is also caused by the action of circumpolar westerly winds in the Southern Ocean, which induce an Ekman transport to the north that is compensated by an upward transport of deep waters (Kuhlbrodt et al, 2007).

The DWF and upwelling waters are connected by a system of surface and deep currents that close the loop. Once the surface waters have penetrated the Atlantic from the Southern Ocean, they cross the Equator northward along the North Brazil current and reach the Gulf Stream, warming up in the process. These warm waters meet the cold and southward current formed at the Labrador Sea in the Grand Banks (Buckley and Marshall, 2016) and separate from the coast flowing eastward. This forms the North Atlantic Current (NAC) which flows both northeastward into the Nordic seas and Arctic Ocean and westward within the subpolar gyre into the Labrador Sea, where NADW is formed. NADW is exported from North Atlantic DWF regions mainly through the Deep Western Boundary Current (DWBC) but also through complex interior pathways that indicate eddy-driven recirculation gyres generated by instabilities of the Gulf Stream (Lozier et al, 1997) and the North Atlantic current system (Lozier, 1999).

The AMOC involves the northward flow of warm, near-surface water across the equator, its cooling, sinking, and then southward flow as NADW, implying a net contribution to the northward ocean heat transport in the Atlantic. The AMOC thus exerts a key influence on the climate of the Northern Hemisphere (NH) through its meridional heat transport. The AMOC is indeed the main reason for the warmer surface waters in the NH compared to those in the Southern Hemisphere (SH), as it accounts for ca. 30% meridional heat transport along the Atlantic (Trenberth and Caron, 2001). Future climate projections robustly indicate a weakening of the AMOC as a consequence both of higher temperatures and an increased meridional freshwater transport into high latitudes in response to global warming (Collins and Knutti, 2013). An AMOC weakening in response to future climate change could partly counterbalance the global warming signal over Europe and Arctic and amplify it over the Tropics (Ortega et al, 2012). On much longer timescales, there is increasing evidence both from the point of view of model studies as well as paleoceanographic reconstructions that AMOC reorganisations underlied the most abrupt climate changes in the recent past (the last glacial period, ca. 110-10 kyr ago) (Lynch-Stieglitz, 2017).

The role of the AMOC in ocean heat transport suggests that AMOC variations can generate ocean heat content anomalies, impacting sea surface temperatures (SSTs), thus potentially driving climate variability at different timescales. This interaction settles an important observed mode of SST variability consisting in a warming/cooling of the North Atlantic on decadal to multidecadal timescales (Knight et al, 2005; Delworth et al, 2007), commonly referred to as the Atlantic Multidecadal Variability (AMV). Its associated spatial pattern of SST anomalies is a basin-wide coherent pattern covering all of the North Atlantic, with the largest anomalies in the subpo-

lar North Atlantic. Its temporal behaviour is described by the AMV index, defined as the basin average SST over the North Atlantic, excluding the externally forced response. This index shows significant low-frequency variability; its power spectrum has the characteristics of red noise, with power increasing with periodicity, and peaks at decadal (20 years) (Chylek et al, 2011, 2012) and multidecadal timescales (40 – 70 years) (Frankcombe et al, 2010). Modeling results linking the AMV to the AMOC are generally based on statistical analyses, and the SST patterns associated with the AMOC considerably differ between models (Buckley and Marshall, 2016, & references therein).

The AMV impacts both regional and global climate (Zhang and Delworth, 2007), including temperatures across North America and Europe (Collins and Sinha, 2003; Sutton and Hodson, 2005; Pohlmann et al, 2006) and North American rainfall (Patricola and Cook, 2013). The AMV can directly impact the passing air masses and thus influence the neighboring continents. The AMV has been reported, e.g., to exert a strong impact on European summer climate (Sutton and Hodson, 2005; Knight et al, 2006). Its warm phase has been also associated with hot and dry summers in southwestern Europe and anomalous low pressure and wet summers in northern Europe (Sutton and Dong, 2012). The AMV is also thought to control low-frequency variations in the position of the Intertropical Convergence Zone (ITCZ), and, in consequence, precipitation over the Sahel region (Folland et al, 1986; Zhang and Delworth, 2006; Ting et al, 2011), and frequency and intensity of Atlantic hurricanes (Knight et al, 2006; Zhang and Delworth, 2007). The ITCZ is a zonally-coherent band of convective precipitation that surrounds the Earth over the Equator. In the annual mean, the ITCZ is located north of the Equator, which is attributed to a warmer NH than the SH because of the net northward AMOC heat transport (Schneider et al, 2014). When the AMOC northward heat transport is intensified, the NH experiences a relative warming with respect to the SH associated with a warm AMV phase, which shifts the ITCZ northward, and vice versa (Green et al, 2017). The AMV can also trigger local responses in atmospheric convection in the tropics, which can influence the Walker circulation and produce remote teleconnections into other ocean basins. For example, the AMV can influence the Pacific basin facilitating the occurrence of ENSO events (Dong et al, 2006). ENSO frequency of occurrence is found to be modulated by the tropical AMV branch, which for positive AMV phases in boreal winter induces La Niña patterns, and more generally a negative phase of the interdecadal Pacific oscillation (IPO) (Ruprich-Robert et al, 2017).

Many modelling studies (Knight et al, 2005, 2006) suggest that the AMOC drives the AMV. Numerous modeling results suggest that AMOC variability is dominated by changes in the Labrador Sea DWF, which is itself sensitive to winter NAO-induced anomalous surface heat flux. The North Atlantic oscillation (or NAO), is an important mode of variability of the atmospheric circulation of the North Atlantic, characterised by a dipole of sea level pressures between the Atlantic high, centered in the Azores Islands, and the polar low centered in Iceland. In these simulations, a positive winter NAO associated with stronger westerlies induces enhanced

surface heat loss and stronger Labrador Sea DWF, leading a positive phase in AMOC and associated AMV by about a decade (Ortega et al, 2017). In addition, observational and modeling studies have shown that a positive AMV (associated with a stronger AMOC) can also induce a negative winter NAO response in the atmosphere, which weakens the Labrador Sea DWF and associated AMOC strength. Hence there might be important coupled interactions between the NAO, AMOC, and the AMV (Zhang et al, 2019, & references therein). Yet, multidecadal AMOC variability may also be affected by changes in the Nordic Seas DWF and associated overflow transport variability, which is not well represented in standard Ocean General Circulation Models (OGCMs), and may not necessarily be dominated by changes in the Labrador Sea deep water formation alone (Smeed et al, 2014, 2018). The influence of the winter NAO on DWF in the Nordic Seas is opposite to that in the Labrador Sea because the former is favored by cold and dry air masses during negative winter NAO associated with fewer storms while the latter is favored by positive winter NAO associated with more storms (Drinkwater et al, 2013).

North Atlantic atmospheric climate variability is dominated at short timescales (monthly and interannual), by the NAO, which is tigthly linked to modulations in the strength and position of the atmospheric jet stream linked in turn to the leading mode of variability of the whole Northern Hemisphere circulation, the annular mode or Arctic Oscillation (AO) (Marshall et al, 2001). The NAO affects the ocean in different ways: changes in the NAO affect the surface wind stress, air-sea heat fluxes,

and SSTs (Bellucci and Richards, 2006). Also, by imposing a white noise signal that is integrated by (Pozo-Vázquez et al, 2001) the ocean creating substantial low-frequency variability (Hasselmann, 1976).

This work will investigate the relationships between the NAO, AMV, the AMOC and the associated teleconnections that are represented in preindustrial control climate simulations with a state of the art coupled climate model. In particular we aim to distinguish the main drivers of AMOC variability and their response to both oceanic and atmospheric influences, to study the link between the AMV and the AMOC, and to analyse the teleconnections of the AMV over the surrounding continents. Two versions of the same coupled climate model at two different resolutions, described in section 2, will be used to investigate the particular effect of this feature in the section 3.

2 Model and experimental design

The model used in this study is the EC-Earth General Circulation Model (GCM) in its coupled version 3.2, maintained and developed by a European Consortium in which the Barcelona Supercomputing Center (BSC) participates and used in the sixth phase of the Coupled Model Intercomparison Project (CMIP6). Two resolutions were considered: a low-resolution version (T255 in the atmosphere and ORCA1L75 in the ocean, which is equivalent to a nominal resolution of 1 in longitude and latitude) and high-resolution version (T511 in the atmosphere and ORCA025L75 in the ocean, equivalent to a nominal resolution of 0.25). They will be referred to as LR and HR in the remainder of the manuscript. Its atmo-

spheric component is the Integrated Forecasting System (IFS), cycle 36r4, of the European Centre for Medium-Range Weather Forecasts (ECMWF) and the ocean component is the version 3.3.1 of the Nucleus for European Modelling of the Ocean (NEMO) (Exarchou et al, 2017). For the sea ice, it uses LIM3, which is embedded in NEMO and is developed at the University of Louvain-La-Neuve (Rousset et al, 2015).

Two control simulations with fixed external forcing conditions from year 1950, each with a different resolution and spanning for 150 years have been used in our analysis. Their first 30 years were excluded due to the present of some model drift, associated with some lingering model adjustment from their spinup phase.

3 Results

3.1 Indices of Interannual to Multidecadal Variability in the North Atlantic

In order to assess North Atlantic interannual to multidecadal variability, we start by investigating the variability of the NAO in both simulations (Fig. 1). The NAO index is computed from sea level pressure data (SLP) during NH winter months (December-February, DJF) as the normalised difference between the standardised SLP in Azores (37.5°N,-2.6°E) and the standardised SLP anomalies in Reykjavik (64.1°N,-21.9°E) (Hurrell, 1995). The time series of both simulations show a certain similarity in scale and amplitude, with strong variations of the NAO index on interannual timescales, which is realistic compared on observational data (Hurrell, 1995).

To investigate how the NAO variability

affects DWF, we analyse the variability of the NH winter mixed layer depth (MLD). We first investigate where MLD variations are largest by assessing the standard deviation of the MLD in the whole North Atlantic in March (Figure 2). The largest values are found in the Nordic Seas, the Irminger Sea and in the Labrador Sea, with maximum values in the latter in both simulations. Therefore we hereafter focus in this area. Figure 3 shows the evolution of the monthly mean value of MLD over the Labrador Sea in March (MLD-LAB). The HR simulation shows a marked low frequency variability with a clear interannual variability. But, while in HR the values remain relatively stable around a mean value of ca. 600 m throughout the 120 years of simulation, the LR simulation shows relatively high values during the first 30 years, reaching a peak during the second decade above 700 m followed by a decrease to values below 200 m.

To understand the differences in MLD-LAB between both simulations, the spatial distribution of the mean of MLD in March of the two simulations is compared (Figure 4). HR shows higher mean values in the Labrador Sea than LR. These differences are clearly associated with differences in the winter sea-ice distribution. In this area, cooling of the relatively saline surface waters increases their density, resulting in a convection, which is reflected in an increase of the MLDs. As long as convection takes place, it contributes to inhibit sea-ice formation, but under weak convection sea-ice formation can overtake, creating a barrier that isolates the ocean from the atmosphere, preventing the heat loss that allows for convection, and resulting in a thinner MLD. This appears to be the case in LR,
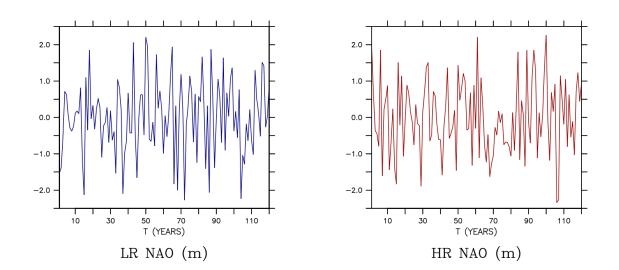
Figure 1: (Left) Timeseries of the interannual North Atlantic Oscillation (NAO) index in winter (DJF) in the LR preindustrial control run. The NAO index is defined as the standardised difference in normalised sea level pressure between Azores and Reykjavik. (Right) The same but for HR preindustrial control run.
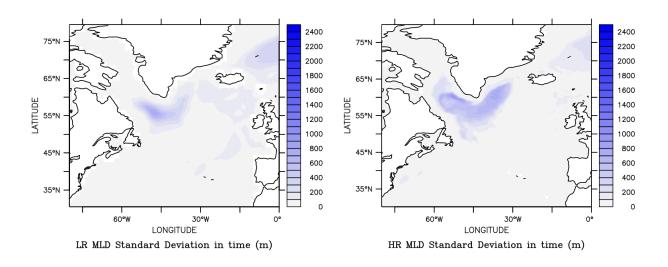

Figure 2: (Left) Spatial map of the long-term standard deviation in the mixed layer depth in March in the LR preindustrial control run, in meters (m). (Right) The same but for the HR preindustrial control run.

where the ice front is located much further south than in HR.

MLD variations are expected to impact the AMOC strength. The latter shows a clear multidecadal variability in both simulations (Figure 5). The largest a.mplitude

Figure 3: (Left) (Left) Timeseries of the monthly mean value of MLD over the Labrador Sea in March in the LR preindustrial control run. (Right) The same but for the HR preindustrial control run.
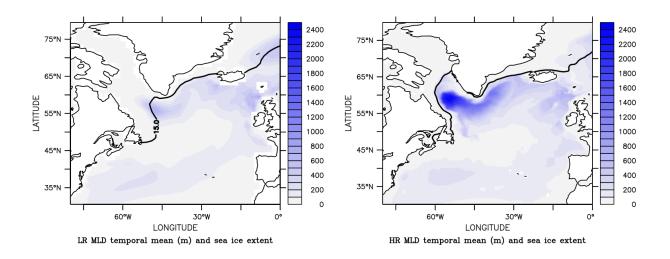

Figure 4: (Left) Spatial map of the mean mixed layer depth in the LR preindustrial control run, in meters (m), and together with the mean March sea-ice front location (black line), defined as the locations where sea-ice concentration equals 15%. (Right) The same but for the HR preindustrial control run

changes are found in LR, where the AMOC initially increases up to its highest value of 16.5 Sv and subsequently decreases, possibly in response to the large MLD-LAB fluctuation in LR. MLD-LAB and AMOC-strength decrease are both possibly related

to the development of a large sea-ice cover inhibiting convection. Despite a slight upward trend, in HR the AMOC shows more constant values, mostly reflecting decadal-scale variability, in agreement with a more stable MLD-LAB with slightly weaker initial values.

The AMOC variations are expected to induce low frequency changes in the AMV, which is herein calculated through the annual mean area-averaged SST anomalies over the North Atlantic basin (between 0°-60°N,80°-0°W) (Sutton and Hodson, 2005) (Figure 6), and filtered with a five-year running mean. Again, there are remarkable differences between the two simulations. As for the AMOC strength, the AMV in LR shows a larger variability than in HR. After reaching its lowest value around year 90 following a large increase to the maximum of the serie in 0.5°C. This large fluctuation does not take place in HR, where there is a clear and well-defined multidecadal variability with a slight upward trend, after a relatively marked interannual variability during the first twenty years of simulation.

3.1.1 Lead-lag correlations

We now quantitatively assess the relations suggested above through the lead-lag cross-correlation of the indices examined above. We start by considering the NAO and the MLD-LAB indices (Figure 7). In both resolutions there is maximum, significant correlation between both indices almost only at lag-zero. This implies MLD-LAB varies in phase with the NAO. This reflects the phased response of MLD-LAB to winds induced by the NAO: strong winds break the stratification inducing mixing. The correlation is weaker in LR, which may reflect

the barrier effect of the larger sea ice cover generated by the model in LR, translating in a weaker impact of NAO on MLD-LAB.

We next analyze the lead-lag cross-correlation netween MLD-LAB and the AMOC index (Figure 8). Both in LR and HR the largest, most significant values between 0.6-0.8 are found at a 3.5-year lag, indicating MLD-LAB variations lead AMOC variations by about 3.5 years: density anomalies generated through mixing propagate into the ocean, subsequently leading to AMOC variations. The correlations are largest for the 5-yr-running mean filtered indices. However, the significance is somewhat lower in correspondence with the lower number of degrees of freedom in the filtered time series, especially in LR.

Finally, the AMOC exerts an influence in the AMV that can also be quantified by their lead-lag cross-correlation (Figure 9). An almost-constant and positive correlation is found between both indices for all lags, most notably in LR. In that simulation the peak at zero-lag means that the AMV and the AMOC vary in phase; the significance in this case only appears for the raw time-series but not in the filtered one. In HR, howerer, significant values are mostly presented at positive lags in normal and filtered series, which means that the AMV response to AMOC can also be delayed up to decadal scales.

3.2 Atmospheric Teleconnections of the AMV

3.2.1 AMV impacts on Surface Air Temperature

We next evaluae the impacts of North Atlantic SST decadal variability (charac-

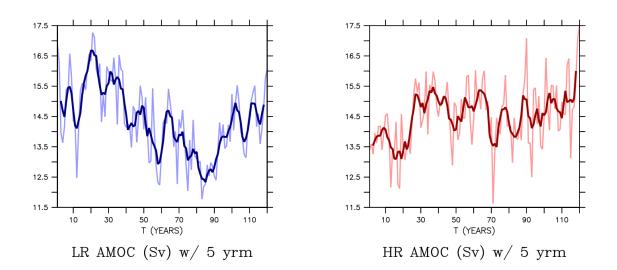LR AMOC (Sv) w/ 5 yrm   HR AMOC (Sv) w/ 5 yrm

Figure 5: (Left) Timeseries of the Atlantic Meridional Overturning Circulation (AMOC) annual averaged at 45-48N in the LR preindustrial control run. The thin blue line represents the interannual AMOC index, and the thick blue line a 5 year low-pass filtered index. (Right) The same but for the HR preindustrial control run.
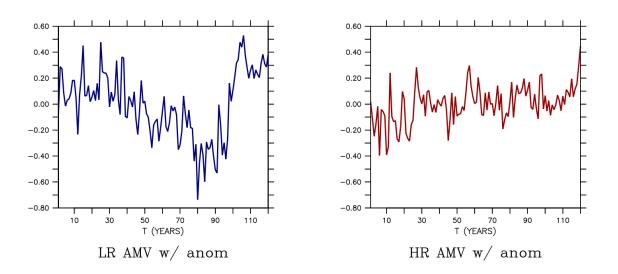

LR AMV w/ anom   HR AMV w/ anom

Figure 6: (Left) Timeseries of the Atlantic Multidecadal Variability (AMV) anomalies averaged in the LR preindustrial control run, calculated as the difference between the AMV index and its long-term mean. (Right) The same but for the HR preindustrial control run.
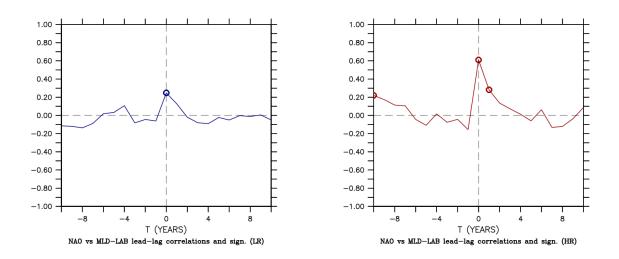
Figure 7: (Left) Lead-lag correlations between the NAO index in DJF and the MLD-LAB index in March in the LR preindustrial control run. Positive (negative) lags indicate that the NAO is leading (lagging) the MLD-LAB. Significant values at a 95% confidence level are highlighted with circles. (Right) The same but for the HR preindustrial control run.
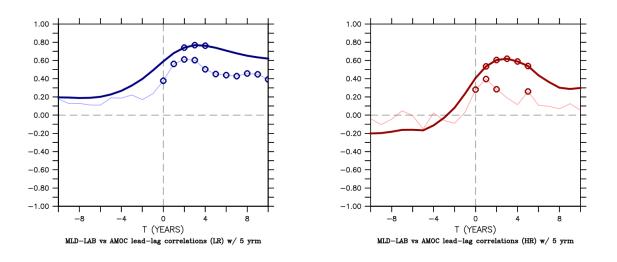

Figure 8: (Left) Lead-lag correlations between the MLD-LAB index in March and the AMOC index in the LR preindustrial control run. Positive (negative) lags indicate that the MLD-LAB is leading (lagging) the AMOC. Significant values at a 95% confidence level are highlighted with circles. (Right) The same but for the HR preindustrial control run.

terised by the AMV) on the climate of the neighboring continents, such as the already

mentioned changes in surface air temperature (TAS) anomalies in North America
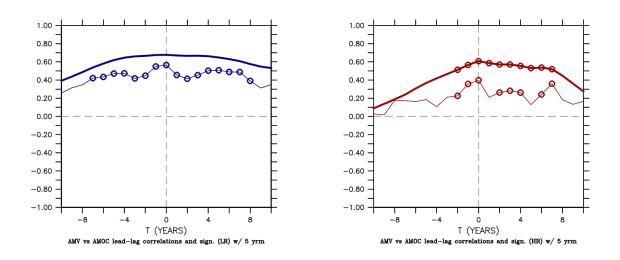
Figure 9: (Left) Lead-lag correlations between the AMV index and the AMOC index in the LR preindustrial control run. Positive (negative) lags indicate that the AMV is leading (lagging) the AMOC. Significant values at a 95% confidence level are highlighted with circles. (Right) The same but for the HR preindustrial control run.

and Europe (Collins and Sinha, 2003; Sutton and Hodson, 2005; Pohlmann et al, 2006; Ting et al, 2011). These impacts are visualized through spatial correlation maps between the AMV index and the TAS 2D fields for both resolutions (Figure 10), allowing us to identify the areas with the greatest correlations, and therefore where the AMV impacts are strongest.

In the North Atlantic large positive correlation values are observed for both resolutions in a tongue-shaped area extending from the Labrador Sea to Western Europe, and then descending through Northwest Africa to the tropical Atlantic (Figure 10). The dots on the map represent grid points where correlations are not significant at the 95% confidence level. This allows us to identify significant correlation values in regions beyond the North Atlantic, especially in the LR simulation. We highlight, for example, a region from the Sahel to the Middle East, the Amazonas basin, and also the equatorial latitudes in the Pacific. The correlations over the Equatorial Pacific become however non-significant when the data are previously smoothed with 5-year running means, to concentrate on the low-frequency variability (Figure 11). This suggests that the influence was exclusive on ENSO, which operates at shorter timescales. All the other impacts identified with the interannual data remain significant with the low-frequency data.

A major difference between LR and HR is that in LR positive significant correlations extending to polar latitudes and also reach Central Europe, while in HR significance over Europe is restricted to the northwest part of the Iberian Peninsula.

To quantify when the impacts over certain regions become more important, we compute lead-lag correlations between the AMV and the spatial TAS averages for
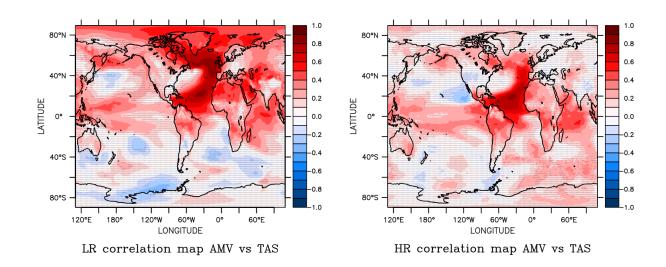
Figure 10: (Left) In-phase correlations between the AMV index and the 2D field of surface air temperature (TAS) in the LR control run. Non-significant values at a 95% confidence level are marked with dots. (Right) The same but for the HR preindustrial control run.
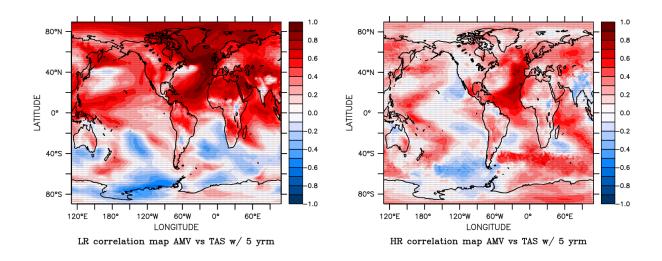

Figure 11: As in Figure 10, but using low-pass filtered data (with a 5-year running mean).

two regions with impacts reported in previous works: North America (20°-70°N,130°-50°W; Figure 12) and western Europe (35°-60°N,10°W-20°E; Figure 13).

In North America the correlation between the AMV and the TAS is especially strong for the LR simulation, with significant values for all lag-times in the unfiltered timeseries. The correlation peaks at 0.6 at zero lag, suggesting that the AMV and the TAS are both in phase. This also occurs in HR with a correlation of only 0.3, and sig-

nificant values only observed for lag -1 (TAS leading) and zero. The correlations of the low-pass filtered indeces help to better detect the lead-lag relationship, by excluding year-to-year climatic noise.

The correlations with the TAS index in Western Europe also show differences between both resolutions, although the differences are not as remarkable as for North America. In the LR unfiltered timeseries there is a positive and significant peak again at lag zero, with a correlation of 0.5 that barely decreases for positive lags. Negative lags have significant but comparatively lower values from lag -1 to -7. The filtered indeces have higher correlations and similar features; maximum of 0.8 at zero lag and a smooth and very slight decline for the positive lags. For the negative lags, the values cease to be significant for the lead year -5. In HR, the maximum and significative values occur in a narrower temporal band, for positive lags from 1 to 4 years. Interestingly, correlations become maximum at lag 3 (with AMV leading), which suggest that in this case the AMV might be the driver of the Western Europe TAS changes.

3.2.2 AMV impacts on precipitations

As discussed in the introduction, the low-frequency changes in the AMV can affect the ITCZ position, thus impacting precipitation on Africa, specifically in the Sahel area (Folland et al, 1986; Zhang and Delworth, 2006; Ting et al, 2011). Spatial correlation maps between the AMV index and the global 2D fields of total precipitation (Figure. 14) show a belt of convective rainfall near the equator, especially in the Pacific in HR, but also in a nar-

rower band in the Equatorial Atlantic. Also in the Atlantic, a band with positive significant correlations is observed between the Iberian Peninsula and the Caribbean Seas. If we focus the study in the Sahelian zone, slight positive correlations are observed along 10°N, although they are not significant. With the low-filtered indexes the correlations are amplified, but not so much their significance (Figure. 15). Some improvement in the correlations appears to emerge in the Sahel in LR, and in the area between Chad and South Sudan in HR.

Focusing on the Sahel, we perform a new lead-lag correlation analysis (Figure. 16). To the end the spatial average of rainfall is calculated in the region 5-20°N and -20-45°E. For the unfiltered timeseries the correlations are significant and positive at lag zero in both resolutions. Specifically in LR, the maximum occurs at lag zero, and correlations barely decrease, remaining significant for most positive lags (i.e. with AMV leading). This is also observed when the indeces are low-pass filtered, with correlation values of up to 0.6 from lag 0 to 5 years, becoming maximum at lag 3 (again indicating that the AMV might be the actual driver). For the HR, correlations are slightly lower than for LR, and in the low-pass filtered data they are non-significant. This is partly reflecting the differences already observed for the spatial correlations **??**, in which largest significant correlations occurred for LR.

4 Conclusions and Discussions

NAO interannual variability induces high frequency changes in the North Atlantic MLD, specially in the Labrador and
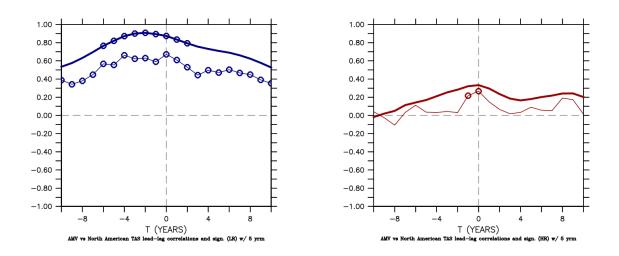
Figure 12: (Left) Lead-lag correlations between the AMV index and the North American TAS index in the LR preindustrial control run. Positive (negative) lags indicate that the AMV is leading (lagging) the TAS in North America. Significant values at a 95% confidence level are highlighted with circles. (Right) The same but for the HR preindustrial control run.
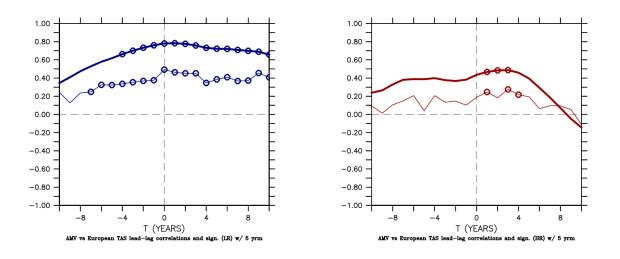

Figure 13: Figure 13: As in Figure 12, but with TAS from Western Europe

Irminger Sea, with NAO and MLD changes in phase. This makes the Labrador Sea a very dynamic area in terms of convection which can impact AMOC variability through density changes. The consequent AMOC changes show multidecadal variability that is led (or lag behind) by the interannual changes in convection. That induced
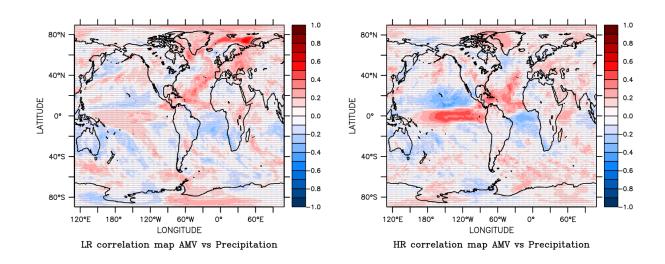
Figure 14: (Left) In-phase correlations between the AMV index and the 2D field of annual mean global precipitations in the LR control run. Non-significant values at a 95% confidence level are marked with dots. (Right) The same but for the HR preindustrial control run.
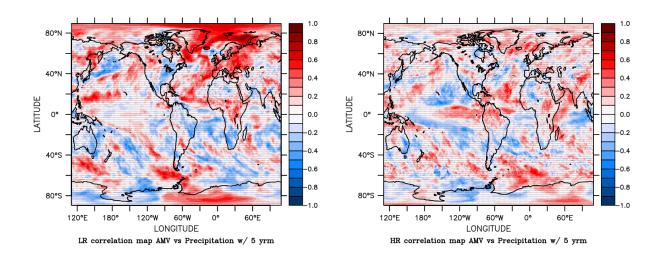

Figure 15: As in Figure 14, but using low-pass filtered data (with a 5-year running mean).

AMOC variability generally lags behind by about 2-5 years.

Because of the impact that AMOC variability has on the ocean heat content, SST are also susceptible to its every change. SST multidecadal variability, characterized by the AMV, is related to AMOC variability in the simulations usually in phase. Despite results like these based on simulations, should be mentioned that no observational study to date has successfully linked SST changes to AMOC variability;
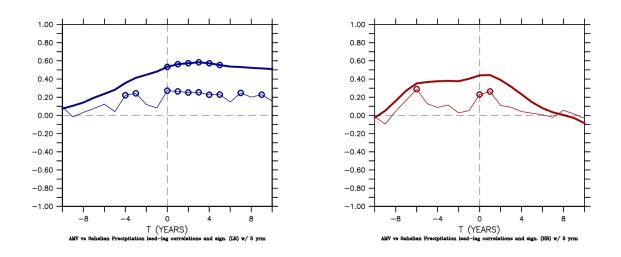
Figure 16: (Left) Lead-lag correlations between the AMV index and the precipitation index in the Sahel in the LR preindustrial control run. Positive (negative) lags indicate that the AMV is leading (lagging) the precipitations in the Sahel. Significant values at a 95% confidence level are highlighted with circles. (Right) The same but for the HR preindustrial control run.

other studies suggest that AMV is driven by other mechanisms. For example, some analyses suggest that both natural and anthropogenic aerosols are behind the large excursions of the AMV (Booth et al, 2012) (Wang et al, 2017). Other analyses suggest that the ocean does not play any role, and that AMV is simply integrating low-frequency stochastic variability from the atmosphere (Clement et al, 2015). However, some other articles suggest that ocean still plays a predominant role over the aerosols (Zhang et al, 2013) which cannot explain the spatial patterns of multi-decadal SST variability and sea surface salinity (SSS) in the North Atlantic ocean. Similarly, other studies (Garuba et al, 2018) conclude that atmospheric fluxes can only excite weak interdecadal variability in the AMV, in contrast with the ocean, which can force strong multidecadal variations.

AMV impacts temperatures and precipitations over the surrounding land masses. When analysed the teleconnections over certain areas, AMV shows statistically significant correlation with temperatures on the most eastern part of North America, and including the midwest, and occidental Europe.

4.1 Main impacts of the resolution

We find clear differences between the two model resolutions. Differences in NAO-driven convection are detected between the resolutions. This is most likely due to the differences in sea ice extent between the two resolutions. The LR simulation generates a too-large, unrealistic ice cover that hampers oceanic deep convection in the Labrador Sea. This does not happen in high res-

olution, where sea ice shows a more realistic extent. Also, in LR the correlations increase with respect to those of the unfiltered indeces, which means that AMV is lagging TAS anomalies. This lag either suggest that there is another mechanism driving both, but influencing first North America, or that there are some methodological artifacts, which could be related to the long-term trends in each timeseries. In HR, all correlation values are non-significant, suggesting that the AMV impact over the region is not reproduced.

The difference between resolutions can also be seen in AMOC variability and its long-term trend. The strong fluctuation of the AMOC in LR along with its multi-decadal behavior is different than in HR, which showed a more constant evolution during most of the integration period. The weakening AMOC is likely driven by the expansion of the sea ice and convection weakening in LR.

The AMV also reflects those long-term fluctuations in LR with a big increase in the penultimate decade. In HR, the AMV shows a more constant multidecadal behaviour, and so teleconnections are also different between the two resolutions. Generally the lower resolution shows higher and more extended correlation values between the AMV and TAS than the HR does. The values are higher in LR than in HR, especially for the smoothed indices. HR usually shows a smaller area of significative values both in Europe and North America, but correlation values still shows that AMV leads both European and North American TAS anomalies in HR.

The main differences for the correlations of unfiltered AMV and precipitation are located in the Barents Sea for LR and

along the Equatorial Pacific for HR simulations. The impact analysis suggests that the resolution can be an important factor when assessing the impacts, and that a proper evaluation in a multi-model context is performed to elucidate if these impacts are model-dependent, and/or resolution-dependent. However, the larger ice cover in LR seems to be excessive and it probably would be the main reason for some of the differences found between resolutions.

This work thus illustrates how the connections and teleconnections within the climate system are sensitive to the model resolution and its simulated mean climate.

Acknowledgements

References

Baines P, Condie S (1998) Observations and modelling of antarctic downslope flows: A review pp 29–49, DOI 10.1029/AR075p0029

Bellucci A, Richards K (2006) Effects of nao

variability on the north atlantic ocean circulation. Geophysical Research Letters 33:2612–, DOI 10.1029/2005GL024890

Booth B, Dunstone N, Halloran P, Andrews T, Bellouin N (2012) Aerosols implicated as a prime driver of twentieth-century north atlantic climate variability. Nature 484:228–32, DOI 10.1038/nature10946

Buckley MW, Marshall J (2016) Observations, inferences, and mechanisms of the atlantic meridional overturning circulation: A review. Reviews of Geophysics 54(1):5–63, DOI 10.1002/2015RG000493

Chylek P, Folland C, Dijkstra H, Lesins G, Dubey M (2011) Ice-core data evidence for a prominent near 20 year timescale of the atlantic multidecadal oscillation. Geophysical Research Letters - GEOPHYS RES LETT 38, DOI 10.1029/2011GL047501

Chylek P, Folland C, Frankcombe L, Dijkstra H, Lesins G, Dubey M (2012) Greenland ice core evidence for spatial and temporal variability of the atlantic multidecadal oscillation. Geophysical Research Letters 39, DOI 10.1029/2012GL051241

Clement A, Bellomo K, Murphy LN, Cane MA, Mauritsen T, Rädel G, Stevens B (2015) The atlantic multidecadal oscillation without a role for ocean circulation. Science 350(6258):320–324, DOI 10.1126/science.aab3980, URL https://science.sciencemag.org/content/350/6258/320, https://science.sciencemag.org/content/350/6258/320.full.pdf

Collins M, Knutti R (2013) Long-term climate change: Projections, commitments and irreversibility pp 1029–1136

Collins M, Sinha B (2003) Predictable decadal variations in the thermohaline circulation and climate. Geophys Res Lett 30, DOI 10.1029/2002GL016504

Delworth T, Zhang R, Mann M (2007) Decadal to centennial variability of the atlantic from observations and models. Geophys Monogr Ser 173:131–148, DOI 10.1029/173GM10

Dong B, Sutton R, Scaife A (2006) Multidecadal modulation of el niño-southern oscillation (enso) variance by atlantic ocean sea surface temperatures. Geophysical Research Letters 33, DOI 10.1029/2006GL025766

Drinkwater K, Miles M, Medhaug I, Otterå OH, Kristiansen T, Sundby S, Gao Y (2013) The atlantic multidecadal oscillation: Its manifestations and impacts with special emphasis on the atlantic region north of 60n. Journal of Marine Systems 133, DOI 10.1016/j.jmarsys.2013.11.001

Exarchou E, Prodhomme C, Brodeau L, Guemas V, Doblas-Reyes F (2017) Origin of the warm eastern tropical atlantic sst bias in a climate model. Climate Dynamics 51, DOI 10.1007/s00382-017-3984-3

Folland C, Palmer T, Parker D (1986) Sahel rainfall and worldwide sea temperatures, 1901–85. Nature 320:602–607, DOI 10.1038/320602a0

Frankcombe L, Heydt AS, Dijkstra H (2010) North atlantic multidecadal climate variability: An investigation of dominant time scales and processes. Journal of Climate 23:3626–3638, DOI 10.1175/2010JCLI3471.1

Garuba O, Lu J, A Singh H, Liu F, Rasch P (2018) On the relative roles of the atmosphere and ocean in the atlantic multidecadal variability. Geophysical Research Letters 45, DOI 10.1029/2018GL078882

Green B, Marshall J, Donohoe A (2017) Twentieth century correlations between extratropical sst variability and itcz shifts. Geophysical Research Letters 44(17):9039–9047, DOI 10.1002/2017GL075044, URL https://agupubs.onlinelibrary.wiley.com/doi/abs/10.1002/2017GL075044, https://agupubs.onlinelibrary.wiley.com/doi/pdf/10.1002/2017GL075044

Hasselmann K (1976) Stochastic climate models part i. theory. Tellus 28(6):473–485, DOI 10.1111/j.2153-3490.1976.tb00696.x, URL https://onlinelibrary.wiley.com/doi/abs/10.1111/j.2153-3490.1976.tb00696.x

Hurrell J (1995) Decadal trends in the north atlantic oscillation. Science (New York, NY) 269:676–9, DOI 10.1126/science.269.5224.676

Knight J, Allan R, Folland C, Vellinga M, Mann M (2005) A signature of persistent natural thermohaline circulation cycles in observed climate. Geophys Res Lett 32, DOI 10.1029/2005GL024233

Knight J, Folland C, Scaife A (2006) Climate impacts of the atlantic multidecadal oscillation. Geophys Res Lett 33, DOI 10.1029/2006GL026242

Kuhlbrodt T, Griesel A, Montoya M, Levermann A, Hofmann M, Rahmstorf S (2007) On the driving processes of the atlantic meridional overturning circulation. Reviews of Geophysics 45(2), DOI 10.1029/2004RG000166

Lozier M (1999) The impact of mid-depth recirculations on the distribution of tracers in the north atlantic. Geophysical Research Letters 26:219–222, DOI 10.1029/1998GL900264, URL https://agupubs.onlinelibrary.wiley.com/doi/abs/10.1029/1998GL900264, https://agupubs.onlinelibrary.wiley.com/doi/pdf/10.1029/1998GL900264

Lozier M, Pratt L, Rogerson A, Miller P (1997) Exchange geometry revealed by float trajectories in the gulf stream. Journal of Physical Oceanography - J PHYS OCEANOGR 27:2327–2341, DOI 10.1175/1520-0485(1997)027⟨2327:EGRBFT⟩2.0.CO;2

Lynch-Stieglitz J (2017) The atlantic meridional overturning circulation and abrupt climate change. Annual Review of Marine Science 9:83–104, DOI 10.1146/annurev-marine-010816-060415

Marshall J, Schott F (1999) Openocean convection: Observations, theory, and models. Reviews of Geophysics 37(1):1–64, DOI 10.1029/98RG02739, URL https://agupubs.onlinelibrary.wiley.com/doi/abs/10.1029/98RG02739

Marshall J, Kushnir Y, Battisti D, Chang P, Czaja A, Dickson R, Hurrell J, McCartney M, Saravanan R, Visbeck M (2001) North atlantic climate variability: phenomena, impacts and mechanisms. International Journal of Climatology

21(15):1863–1898, DOI 10.1002/joc.693, URL https://rmets.onlinelibrary.wiley.com/doi/abs/10.1002/joc.693

Ortega P, Montoya M, González Rouco JF, Mignot J, Legutke S (2012) Variability of the atlantic meridional overturning circulation in the last millennium and two ipcc scenarios. Climate Dynamics - CLIM DYNAM 38:1–23, DOI 10.1007/s00382-011-1081-6

Ortega P, Guilyardi ÉN, Swingedouw D, Mignot J, Nguyen S (2017) Reconstructing extreme AMOC events through nudging of the ocean surface: a perfect model approach. Climate Dynamics pp 1–17, DOI 10.1007/s00382-017-3521-4, URL http://hal.upmc.fr/hal-01449390

Patricola C, Cook K (2013) Mid-twenty-first century climate change in the central united states. part ii: Climate change processes. Climate Dynamics 40(3):569–583, DOI 10.1007/s00382-012-1379-z

Pohlmann H, Sienz F, Latif M (2006) Influence of the multidecadal atlantic meridional overturning circulation variability on european climate. Journal of Climate - J CLIMATE 19, DOI 10.1175/JCLI3941.1

Pozo-Vázquez D, Esteban-Parra MJ, Rodrigo F, Castro-Díez Y (2001) A study of nao variability and its possible non-linear influences on european surface temperature. Climate Dynamics 17:701–715, DOI 10.1007/s003820000137

Rousset C, Vancoppenolle M, Madec G, Fichefet T, Flavoni S, Barthélemy A, Benshila R, Chanut J, Levy C, Masson S, Vivier F (2015) The louvain-la-neuve sea ice model lim3.6: global and regional capabilities. Geoscientific Model Development 8(10):2991–3005, DOI 10.5194/gmd-8-2991-2015, URL https://www.geosci-model-dev.net/8/2991/2015/

Ruprich-Robert Y, Msadek R, Castruccio F, Yeager S, Delworth T, Danabasoglu G (2017) Assessing the climate impacts of the observed atlantic multidecadal variability using the gfdl cm2.1 and ncar cesm1 global coupled models. Journal of Climate 30(8):2785–2810, DOI 10.1175/JCLI-D-16-0127.1, URL https://doi.org/10.1175/JCLI-D-16-0127.1, https://doi.org/10.1175/JCLI-D-16-0127.1

Schneider T, Bischoff T, Haug G (2014) Migrations and dynamics of the intertropical convergence zone. Nature 513:45–53, DOI 10.1038/nature13636

Smeed DA, McCarthy GD, Cunningham SA, Frajka-Williams E, Rayner D, Johns WE, Meinen CS, Baringer MO, Moat BI, Duchez A, Bryden HL (2014) Observed decline of the atlantic meridional overturning circulation 2004ndash;2012. Ocean Science 10(1):29–38, DOI 10.5194/os-10-29-2014, URL https://www.ocean-sci.net/10/29/2014/

Smeed DA, Josey SA, Beaulieu C, Johns WE, Moat BI, Frajka-Williams E, Rayner D, Meinen CS, Baringer MO, Bryden HL, McCarthy GD (2018) The north atlantic ocean is in a state of reduced overturning. Geophysical Research Letters 45(3):1527–1533, DOI 10.1002/2017GL076350, URL https://agupubs.onlinelibrary.wiley.com/doi/abs/10.1002/2017GL076350

Sutton RT, Dong B (2012) Atlantic ocean influence on a shift in european climate in the 1990s. Nature Geoscience 5:788–792, DOI 10.1038/ngeo1595

Sutton RT, Hodson DLR (2005) Atlantic ocean forcing of north american and european summer climate. Science 309(5731):115–118, DOI 10.1126/science.1109496, URL https://science.sciencemag.org/content/309/5731/115, https://science.sciencemag.org/content/309/5731/115.full.pdf

Ting M, Kushnir Y, Seager R, Li C (2011) Robust features of atlantic multidecadal variability and its climate impacts. Geophysical Research Letters - GEOPHYS RES LETT 38, DOI 10.1029/2011GL048712

Trenberth K, Caron J (2001) Estimates of meridional atmosphere and ocean heat transports. J Climate 14:3433–3443, DOI 10.1175/1520-0442(2001)014⟨3433:EOMAAO⟩2.0.CO;2

Wang J, Yang B, Ljungqvist F, Luterbacher J, Osborn T, R Briffa K, Zorita E (2017) Internal and external forcing of multidecadal atlantic climate variability over the past 1,200 years. Nature Geoscience 10:512–518, DOI 10.1038/ngeo2962

Zhang R, Delworth T (2006) Impact of atlantic multidecadal oscillations on india/sahel rainfall and atlantic hurricanes. Geophys Res Lett 33, DOI 10.1029/2006GL026267

Zhang R, Delworth T (2007) Zhang, r. delworth, t. l. impact of the atlantic multidecadal oscillation on north pacific climate variability. geophys. res. lett. 34,

l23708. Geophysical Research Letters - GEOPHYS RES LETT 34, DOI 10.1029/2007GL031601

Zhang R, Delworth TL, Sutton R, Hodson DLR, Dixon KW, Held IM, Kushnir Y, Marshall J, Ming Y, Msadek R, Robson J, Rosati AJ, Ting M, Vecchi GA (2013) Have aerosols caused the observed atlantic multidecadal variability? Journal of the Atmospheric Sciences 70(4):1135–1144, DOI 10.1175/JAS-D-12-0331.1, URL https://doi.org/10.1175/JAS-D-12-0331.1

Zhang R, Sutton R, Danabasoglu G, Kwon YO, Marsh R, Yeager S, E Amrhein D, Little C (2019) A review of the role of the atlantic meridional overturning circulation in atlantic multidecadal variability and associated climate impacts. Reviews of Geophysics DOI 10.1029/2019RG000644